

Method Article

Standardized method for controlled modification of poly (ethylene terephthalate) (PET) crystallinity for assaying PET degrading enzymes



Thore Bach Thomsen, Cameron J. Hunt, Anne S. Meyer*

Department of Biotechnology and Biomedicine, Protein Chemistry and Enzyme Technology Section, DTU Bioengineering,
Technical University of Denmark, Kgs., Lyngby 2800, Denmark

ABSTRACT

Poly(ethylene terephthalate) (PET) is a polyester plastic, which is widely used, notably as a material for single-use plastic bottles. Its accumulation in the environment now poses a global pollution threat. A number of enzymes are active on PET providing new options for industrial biorecycling of PET materials. The enzyme activity is strongly affected by the degree of PET crystallinity (X_C), and the X_C is therefore a relevant factor to consider in enzyme catalyzed PET recycling. Here, we present a new experimental methodology, based on systematic thermal annealing for controlled preparation of PET disks having different X_C , to allow systematic quantitative evaluation of the efficiency of PET degrading enzymes at different degrees of PET substrate crystallinity. We discuss the theory of PET crystallinity and compare PET crystallinity data measured by differential scanning calorimetry and attenuated Fourier transform infrared spectroscopy.

- This study introduces a simple method for controlling the crystallinity of PET samples via annealing in a heat block.
- The present methodology is not limited to the analytical methods included in the methods details.

© 2022 The Author(s). Published by Elsevier B.V.
This is an open access article under the CC BY-NC-ND license
(<http://creativecommons.org/licenses/by-nc-nd/4.0/>)

ARTICLE INFO

Method name: Standardized method for controlled modification of poly(ethylene terephthalate) (PET) crystallinity for assaying PET degrading enzymes

Keywords: PET hydrolase, PET crystallinity, Enzyme assay

Article history: Received 12 April 2022; Accepted 4 August 2022; Available online xxx

DOI of original article: [10.1016/j.nbt.2022.02.006](https://doi.org/10.1016/j.nbt.2022.02.006)

* Corresponding author.

E-mail address: asme@dtu.dk (A.S. Meyer).

Specifications table

Subject Area:	Chemical Engineering
More specific subject area:	Enzyme Technology
Method name:	Standardized method for controlled modification of poly(ethylene terephthalate) (PET) crystallinity for assaying PET degrading enzymes
Name and reference of original method:	N/A
Resource availability:	N/A

Method details

Background: Polyethylene terephthalate as an enzyme substrate

Poly(ethylene terephthalate) (PET) is a synthetic polyester used in packaging materials and plastic bottles. PET accounts for ~7% of global plastic usage [1], and is a key contributor to the increasing plastic pollution [2]. The polymeric chains of PET consist of repeating units of ethylene glycol and terephthalic acid linked together by ester bonds. These polymer chains are either in an amorphous state (absence of long-range molecular order) or in a crystal structure (highly ordered) [3].

The degree of crystallinity (X_C) of a PET sample refers to the fraction of the total polymer chains being in the crystal structure state. The X_C is a result of the PET process history, as crystallization is induced either thermally, at temperatures above the glass transition temperature T_g (T_g is 76°C for amorphous PET), or during certain mechanical operations [4,5]. The amorphous fraction of PET is in fact comprised of two fractions, namely a rigid amorphous fraction (RAF) and a mobile amorphous fraction (MAF); the ratio of each is written as X_{RAF} and X_{MAF} , respectively. The RAF is present at the interface between the crystal and the amorphous regions as an immobilized phase caused by the crystallization, and the mobility of RAF is more restrained than the completely amorphous region MAF. The X_{RAF} of a PET sample increases with the X_C , while X_{MAF} decreases [6,7].

Although PET is a synthetic polymer, recent data have shown that certain esterolytic enzymes (EC 3.1.1.x), including the PET hydrolase from the bacterium *Ideonella sakaiensis* 201-F6, originally specified as a PETase (or IsPETase) [8], now classified as EC 3.1.1.101, are capable of catalyzing hydrolysis of the ester bonds within PET. The activity of these enzymes are, however, limited on PET samples with a high X_C [9–12]. X_C of PET in water bottles ranges from 21–31% [13] making the significance of X_C on PET degrading enzyme activity of critical importance in biobased industrial PET recycling.

Here we present the practical details and the theory behind an experimental methodology that we have developed for preparing PET samples of different degrees of crystallinity, X_C , to allow systematic evaluation of the efficiency of PET degrading enzymes in response to the X_C of PET [11]. We introduce annealing involving controlled heating and isothermal cold crystallization to control the X_C of standardized PET sheets (Fig. 1).

Substrate preparation

Preparation of PET material

Amorphous or low crystalline PET films or sheets (e.g. 1 mm thick amorphous PET cat. No. ES30301 from Goodfellow Cambridge Ltd, Huntingdon, UK) are used as starting material to obtain PET materials having different X_C via annealing and isothermal cold crystallization. The PET material is cut into uniform disks using a generic hole punch (\varnothing 6mm), prior to annealing. Although the starting materials are categorized as amorphous PET materials, it is important to note that the crystallinity of the PET films and sheets differ, and observe that they are not completely amorphous (see Method Validation, below).

Annealing and isothermal cold crystallization of PET

The X_C of the PET discs is systematically altered via annealing followed by cold crystallization as follows: A PET disk is transferred into a 2 mL Eppendorf tube and annealed in a heating block at

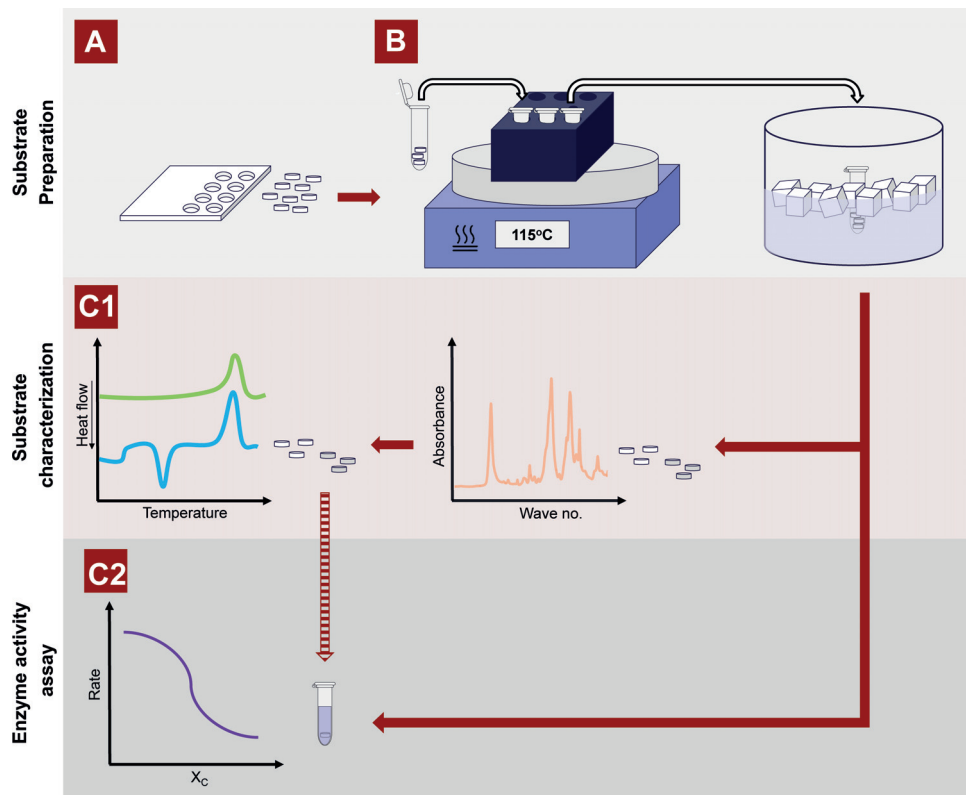


Fig. 1. Schematic representation of the method presented in this paper. (A) Amorphous PET material is cut into disks (\varnothing 6mm) using a hole punch. (B) The disks are transferred into a 2 mL Eppendorf tube, and annealed at 115°C for a specified period of time to induce crystal formation via cold crystallization. The crystallization is quenched by cooling the annealed sample in ice water. The annealed PET samples are then analyzed by ATR-FTIR to quantify X_{MAF} , and/or identify contaminants. The samples used for ATR-FTIR may be used directly for reaction or other analyses, including: (C1) DSC analysis for further characterization of substrate properties such as X_c or (C2) enzymatic reactions for quantifying the effect of substrate X_c for a specific PET degrading enzyme.

115°C for a defined amount of time (minutes); up to three disks can be added per Eppendorf tube, still achieving the same crystallization result as if only one disk is added at a time. The crystallization of the annealed PET sample is quenched by immediately transferring the Eppendorf tube into an ice water bath. It is kept on ice for at least 30 sec to ensure that the crystallized sample has been sufficiently cooled. “Untreated” samples to be used for comparison should be annealed at 85°C for 5 min to remove the enthalpy relaxation caused by the aging of the polymer [14].

Substrate characterization

Quantification of X_{MAF} by ATR-FTIR

Attenuated total reflection Fourier-transform infrared spectroscopy (ATR-FTIR) does not require any substrate preparation and can thus be performed directly on the PET disks after annealing. As it is a non-destructive method, the samples analyzed by ATR-FTIR can be used for further analysis, such as differential scanning calorimetry (DSC) or enzymatic treatment.

The peaks of interest described in this paper are at 973 cm^{-1} and 898 cm^{-1} . These two peaks are associated with the *trans* (973 cm^{-1}) and *gauche* (898 cm^{-1}) conformer of ethylene glycol [14,15]. While the *gauche* conformer is only associated with amorphous PET the *trans* conformer is present

in both the crystalline and amorphous regions [14]. The ratio of the absorbances at these two peaks (A_{973}/A_{898}) is proportional with the X_{MAF} of the sample.

Quantification of the X_C and X_{MAF} by DSC

DSC can be used to quantify the X_C of a sample annealed for a specific period of time, by analyzing a few samples ($n=3$) from the batch. A temperature range from 20°C to 270°C is sufficient to determine the thermal features required to estimate X_C and X_{MAF} of PET samples. A constant heating rate of 10°C min⁻¹ is recommended, as some thermal features are dependent on the heating rate [9,11,16]. The X_C of a PET sample, measured by DSC, is then calculated according to Eq. (1):

$$X_C = \frac{\Delta H_m - \Delta H_{cc}}{\Delta H_m^0} \cdot 100\% \quad (1)$$

Here, ΔH_{cc} is the cold crystallization enthalpy (numerical value) of the sample, ΔH_m is the heat of melting of the sample, and ΔH_m^0 is the heat of melting of a pure crystalline sample. According to literature ΔH_m^0 is 140 J g⁻¹ [17].

The X_{MAF} is calculated according to Eq. (2):

$$X_{MAF} = \frac{\Delta C_{P(m)}}{\Delta C_{P(a)}} \quad (2)$$

Where $\Delta C_{P(m)}$ is the change in heat capacity of the sample at T_g and $\Delta C_{P(a)}$ is the change in heat capacity at T_g of a completely amorphous sample. By extrapolation from a linear regression curve of measured $\Delta C_{P(m)}$ values and X_C of PET disk samples we have previously estimated $\Delta C_{P(a)}$ of an amorphous PET disk sample to be approximately 0.47 J g⁻¹ K⁻¹ [11].

Enzyme assay

The effect of the increased substrate crystallinity on the particular enzyme activity is evaluated on PET disks of different X_C by measuring the concentration of soluble products formed during enzymatic reaction. Products are measured in terms of bis(2-hydroxyethyl)-terephthalic acid (BHET) equivalents via absorbance measurements of the reaction at 240 nm [18]. The rate of the product formation is then plotted against X_C of the PET disks used.

The enzyme reactions are performed in Eppendorf tubes using 1 disk and a reaction volume of 1 mL in buffer. During the enzymatic treatment, 10µL of the reaction is sampled at various time points. The concentration of soluble product should be normalized with respect to the starting volume V_0 according to Eq. (3).

$$C_i = \frac{C_{s,i} * V_i + \sum_{i=1}^n (C_{s,n} * V_{s,n})}{V_0} \quad (3)$$

Where C_i and V_i is the normalized concentration of soluble products and the reaction volume at time point i . $C_{s,i}$, $C_{s,n}$, and $V_{s,n}$ is the measured concentration of soluble products in the sample measured at time point i or n and the sampling volume at time point n .

The product release rate on each PET sample is then calculated from the linear regions of the progress curves. The rate data are then plotted against the X_C or X_{MAF} quantified by either DSC or ATR-FTIR.

Method validation (Case study)

Materials and instrumentation

PET material

1 mm thick amorphous PET sheets (Cat. No. ES303010) denoted as PET-S, 250 µm thick amorphous PET film (Cat. No. ES301445) denoted as PET-F, and semi-crystalline PET particles, Ø<300µm (Cat. No. ES306031), denoted as PET-P were all from Goodfellow (Cambridge Ltd, Huntingdon, UK). The PET-P particles were cast into an amorphous PET sheet by melting 0.5 g of particles in an aluminum dish

(\varnothing 2.6 cm) for 1 min at 270°C and subsequent quenching in ice water. These latter samples will be denoted as PET-C. Starting crystallinity was measured to be: PET-S: $9.1 \pm 1.3\%$, PET-F: $1.3 \pm 0.4\%$, PET-P: $37.5 \pm 0.7\%$.

Isothermal crystallization

PET-S, PET-F, and PET-C were all cut into disks using a generic hole punch (\varnothing 6mm). Samples were annealed at 115°C for 5, 6, 7, 8, 9, 10, 12, 15 min (PET-S, PET-F), and for 30 min (PET-S, PET-F, and PET-C) in a heating block. At the specific time points the samples were quenched (cold crystallized), by transferring the annealed samples into ice water for 30 sec. "Untreated" PET samples were annealed at 85°C for 5 min, and subsequently quenched in ice water for 30 sec.

ATR- FTIR analysis

ATR-FTIR was performed directly on the PET disks ($n=3$) using a Spectrum 100 FTIR spectrometer (PerkinElmer, MA, USA). Samples were monitored from 4000 to 650 cm^{-1} with a resolution of 4 cm^{-1} . Each spectrum consisted of an average of 4 scans.

DSC analysis

The X_C of the PET samples was quantified using DSC measurements ($n=3$) on a Pyris 1 Calorimeter (Perkin Elmer, Waltham, Massachusetts, USA). A constant heating rate of 10°C min^{-1} was applied on samples weighing 8.5 ± 0.5 mg for PET-P and PET-S or 6.5 ± 0.5 mg for PET-F between temperatures of 20°C and 270°C. X_C and X_{MAF} was calculated according to Eqs. (1) and (2), respectively.

Enzymes

LCC_{ICCG} was expressed recombinantly in *E. coli* Shuffle T7 and purified as described in [11] (Expression also works in *E. coli* BL21 (DE3) cells).

Enzyme activity assay

1 disk of PET was treated with 150 nM LCC_{ICCG} in 1 mL 0.5M glycine-NaOH buffer pH 9 at 70°C during shaking in a thermomixer (Eppendorf, Hamburg, Germany) for up to 8 h. 10 μL were sampled at specific time points during the reaction. The product formation, at the time points, was quantified by measuring the absorbance at 240 nm using a Synergy HT™ plate reader (BioTek, Winooski, Vermont, United States) as described in [18]. A sample containing 32.6 mg/mL PET-P, corresponding to the average weight of a PET-S disk, was included as a benchmark and assayed under the same conditions as PET-S. All reactions were performed in triplicate.

Results validation

The increase in X_C caused by the annealing followed the characteristic Avrami equation (Fig. 2A), which is associated with crystal growth during annealing [19,20] and the X_C data obtained per annealing time were higher for the PET-S (sheet) than the PET-F (film) samples (Fig. 2A).

As a supplement to the DSC measurements the ATR-FTIR spectra of the untreated PET samples and extensively annealed PET samples (heated for 30 min at 115°C), respectively, were obtained for the PET-C, PET-F, and PET-S. From the ATR-FTIR spectra, it was observed that the peak at 973 cm^{-1} increased upon annealing while the absorbance at 898 cm^{-1} decreased for both the PET-S and the PET-C samples. A non-linear relationship was observed between the X_C and the A_{973}/A_{898} ratio of PET-S (linear model $r^2 = 0.96$) (Fig. 2C), but a linear correlation, $r^2 = 0.99$, was observed between the X_{MAF} and A_{973}/A_{898} ratio (Fig. 2D). These observations are in agreement with the *gauche* conformation only being present in X_{MAF} . For PET-S, ATR-FTIR can thereby be used as a non-destructive method to directly quantify the X_{MAF} of thermally annealed samples before enzymatic treatment.

It is important to note that no changes were observed on the ATR-FTIR spectrum of the PET-F samples. Moreover, both the untreated and annealed PET-F samples produced a broad peak with absorbance maximum at 955 cm^{-1} . We attribute these data to the possible presence of impurities in the original PET film. For this reason, PET-S is recommended as a substrate for the method presented here for quantification of the effect of X_C on the product release rate of PET degrading enzymes.

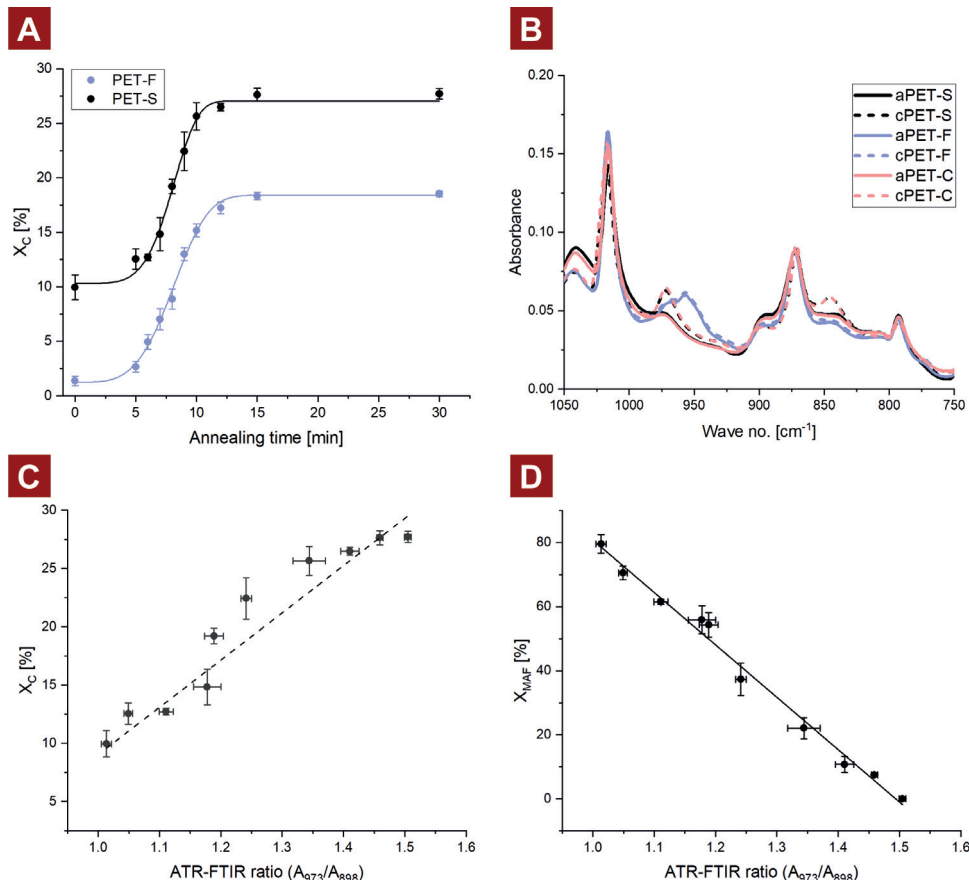


Fig. 2. Characterization of PET samples ($n=3$) annealed at 115°C. (A) Change in the degree of crystallinity (X_C), measured by DSC of amorphous PET-P (light blue dots) and PET-S (black dots) as a function of annealing time at 115°C. The bold lines represent a nonlinear curve fit to a modified version of the Avrami equation. (B) ATR-FTIR spectrum of PET-C (light red), PET-F (light blue), and PET-S (black lines) which are either untreated (solid lines) or cold crystallized (dashed lines) at 115° for 30 min. (C) Correlation (non-linear) between the X_C measured by DSC and the ATR-FTIR ratio A_{973}/A_{898} ; the dotted line is included only as an aid for the eye. (D) Linear correlation between the X_{MAF} measured by DSC and the ATR-FTIR ratio A_{973}/A_{898} .

From the enzymatic reaction progress curves it was evident that the product release rate catalyzed by LCC_{ICCG} on the untreated sample ($X_C=8.2\%$) was constant throughout the 8 h of the enzymatic treatment (Fig. 3A). A lag phase was evident for the samples with higher X_C [11]. The substrate X_C , induced by annealing affected the length of the observed lag phases, which increased with an increasing substrate crystallinity. The samples with a low X_C (9.3 and 13.8%) thus also displayed lag phases, although the product release rate did not differ once a steady-state reaction rate had been reached. Once a steady-state was reached for the samples with 9.3 or 13.8% X_C (determined by the linear region of the progress curves displayed in Fig. 3A), it was observed that the product release rate of these samples had reached the same level as the untreated sample. In contrast, the samples with a X_C of 18.8 % or higher displayed significantly lower product release rates.

The correlation between the product release rate and the X_C followed a sigmoidal trend (Fig. 3B). This indicates that the negative effect on the LCC_{ICCG} catalyzed product release rate caused by increasing substrate crystallinity, reached a critical point at a X_C between 13.8 and 18.8%, as the reaction rate decreased ~10 fold within this range. A similar observation was made for the *Ideonella sakaiensis* PETase, IsPETase, using PET-F samples crystallized via non-isothermal crystallization from melt [10].

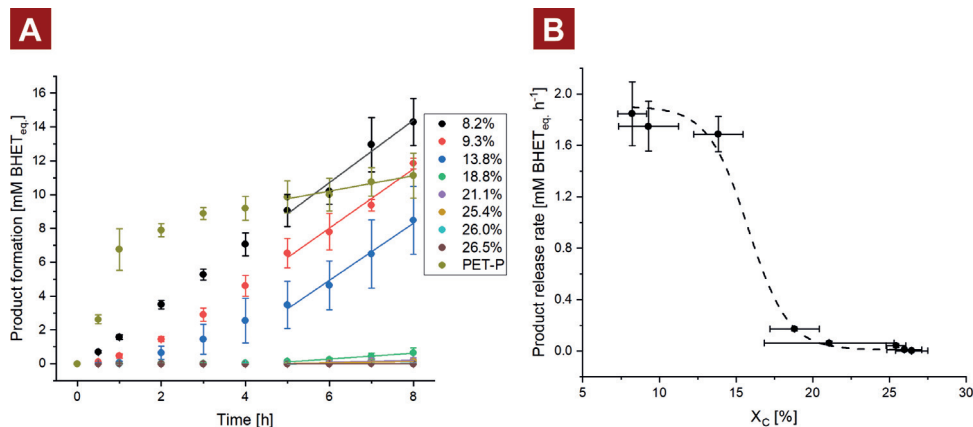


Fig. 3. Enzymatic degradation of PET-S samples with various degrees of crystallinity. (A) Progress curves made by continuous sampling of PET samples ($n=3$) using 150 nM LCC_{ICCG} in 50 mM Glycine-NaOH pH 9 at 70°C. A sample containing 32.6 mg/mL of highly crystalline PET-P ($X_C = 37.5 \pm 0.7\%$) was included as a reference. (B) Product release rate of LCC_{ICCG} against the substrate crystallinity. The rates were calculated based on the linear regions from Fig. 3A).

Important considerations

The annealing temperature affects the crystallization rates, X_C at saturation/metastable state, and the crystal thickness [7]. The annealing temperature of 115°C was chosen as X_C saturation was reached within a reasonable amount of time [11]. The enzyme response data (Fig. 3B) underline that it is particularly important to evaluate the reaction rates based on progress curves rather than on end-point measurements. Although PET hydrolase activity as EC 3.1.1.101 has now been defined as producing mono(2-hydroxyethyl) terephthalate (MHET) and (ethylene terephthalate)_{n-1} from (ethylene terephthalate)_n (www.BRENDA-enzymes.org), it is known that many PET degrading (poly)esterases, including the *I. sakaiensis* PETase, produce some BHET in addition to MHET [18,21] measurable by HPLC. In the present method, we employed direct spectrophotometry of supernatant samples at 240 nm, principally as described in [18]. This quantification of the products as BHET_{eq} is thus mainly a method for enzyme screening or for assessing e.g. the significance of systematic substrate alterations.

A sample containing 32.6 mg of PET-P, corresponding to the average mass of a PET-S disk, was included as a benchmark. The X_C of PET-P was very high ($37.5 \pm 0.7\%$), while the total surface area of the PET-P sample was several fold larger than that of a PET-S disc (according to our calculations minimum 6 times larger considering a particle diameter of 300 μm of each PET-P particle). During the initial 1.5 h of incubation, the initial product release rate on the PET-P was significantly higher than the low crystalline PET-S sample. After this point (after an extent of reaction of approximately 4%) the product release rate decreased 14 fold, from $7 \pm 0.9 \text{ mM BHET}_{\text{eq}} \cdot \text{h}^{-1}$ to $0.5 \pm 0.03 \text{ mM BHET}_{\text{eq}} \cdot \text{h}^{-1}$. This observed leveling off with time agrees with other studies and appears to be a common trait of enzymatic PET degradation [9,11,12]. Based on recording a large variation in the enzymatic degradability of PET chips from different parts of postconsumer packaging material, it has been suggested [9], that differences in degradability may be due to differences in the distribution of the crystalline microstructures within heterogeneous PET samples. Our data on PET-P versus PET-S (Fig. 3) agree with this interpretation. Taken together, the results underline the importance of annealing the PET disks in a controlled manner to examine the significance of crystallinity on PET hydrolase degradation rates.

Conclusion

In this study, we present a new methodology used to quantitatively evaluate the influence of PET substrate crystallinity, X_C , on the action of PET degrading enzymes. The method involves the

preparation of PET samples having different levels X_C , by annealing PET samples above their T_g using commercially available PET sheets as starting material.

As a validation of the methodology the effect of the X_C , on the product release rate of the gold standard thermostable PET-hydrolyzing enzyme LCC_{ICCG} was investigated. The findings showed that the enzymatic rate was heavily dependent on the X_C . Especially between a X_C of 13.8 and 18.8%, at which the reaction rate decreased ~10 fold. Furthermore, it was observed that the product release rates were not constant during the reaction using PET at a $X_C > 8.2\%$. The data thus emphasize the importance of using progress curves rather than end-point measures when evaluating the catalytic efficiency of PET degrading enzymes on PET, and notably on PET substrate samples of different X_C .

It is suggested that the methodology presented in this paper is used as a standardized methodology for addressing the influence of X_C on PET degrading enzymes to allow a direct comparison between different studies.

Perspectives

As a final remark, it is important to state that this methodology is not limited to the characterization of the influence of X_C on the enzyme activity. An alternate annealing temperature (above T_g) may be used. This will, however, result in different crystallization rates, X_C at saturation/metastable state, and crystal thickness. The thermally annealed PET samples may also be used in other enzyme assays, which are addressing different properties than the product release rate.

Declaration of Competing Interest

The authors declare that they have no known competing financial interests or personal relationships that could have appeared to influence the work reported in this paper.

Data availability

Data will be made available on request.

Acknowledgements

Funding from The H.C. Ørsted Cofund Postdoc Program, Technical University of Denmark, and DTU Bioengineering, Technical University of Denmark,

References

- [1] European Commission. A circular economy for plastics – Insights from research and innovation to inform policy and funding decisions. 2019. doi:[10.2777/269031](https://doi.org/10.2777/269031).
- [2] World Economic Forum Ellen MacArthur Foundation McKinsey & Company. The New Plastics Economy: Rethinking the future of plastics. 2016.
- [3] Mitchell G.R., Tojeira A. Controlling the morphology of polymers: multiple scales of structure and processing. 2016. doi:[10.1007/978-3-319-39322-3](https://doi.org/10.1007/978-3-319-39322-3).
- [4] N. Sun, J. Yang, D. Shen, The effect of water absorption on the physical ageing of amorphous poly(ethylene terephthalate) film, Polymer 40 (1999) 6619–6622 (Guildf), doi:[10.1016/S0032-3861\(99\)00246-3](https://doi.org/10.1016/S0032-3861(99)00246-3).
- [5] S. Mandal, A. Dey, PET chemistry, in: Recycling Polyethylene Terephthalate Bottles, Elsevier, 2019, pp. 1–22, doi:[10.1016/b978-0-12-811361-5.00001-8](https://doi.org/10.1016/b978-0-12-811361-5.00001-8).
- [6] R. Androsch, B. Wunderlich, The link between rigid amorphous fraction and crystal perfection in cold-crystallized poly(ethylene terephthalate), Polymer 46 (2005) 12556–12566, doi:[10.1016/j.polymer.2005.10.099](https://doi.org/10.1016/j.polymer.2005.10.099).
- [7] R. Rastogi, W.P. Vellinca, S. Rastogi, C. Schick, H.E.H. Meijer, The three-phase structure and mechanical properties of poly(ethylene terephthalate), J. Polym. Sci. Part B Polym. Phys. 42 (2004) 2092–2106, doi:[10.1002/polb.20096](https://doi.org/10.1002/polb.20096).
- [8] S. Yoshida, K. Hiraga, T. Takehana, I. Taniguchi, H. Yamaji, Y. Maeda, et al., A bacterium that degrades and assimilates poly(ethylene terephthalate), Science 351 (2016) 1196–1199, doi:[10.1126/science.aad6359](https://doi.org/10.1126/science.aad6359).
- [9] R. Wei, D. Breite, C. Song, D. Gräsing, T. Ploss, P. Hille, et al., Biocatalytic degradation efficiency of postconsumer polyethylene terephthalate packaging determined by their polymer microstructures, Adv. Sci. 6 (2019), doi:[10.1002/advs.201900491](https://doi.org/10.1002/advs.201900491).
- [10] E. Erickson, T.J. Shakespeare, F. Bratti, B.L. Buss, R. Graham, M.A. Hawkins, et al., Comparative performance of PETase as a function of reaction conditions, substrate properties, and product accumulation, ChemSusChem 15 (2022), doi:[10.1002/cssc.202101932](https://doi.org/10.1002/cssc.202101932).

- [11] T.B. Thomsen, C.J. Hunt, A.S. Meyer, Influence of substrate crystallinity and glass transition temperature on enzymatic degradation of polyethylene terephthalate (PET), *New Biotechnol.* 69 (2022) 28–35, doi:[10.1016/j.nbt.2022.02.006](https://doi.org/10.1016/j.nbt.2022.02.006).
- [12] V. Tournier, C.M. Topham, A. Gilles, B. David, C. Folgoas, E. Moya-Leclair, et al., An engineered PET depolymerase to break down and recycle plastic bottles, *Nature* 580 (2020) 216–219, doi:[10.1038/s41586-020-2149-4](https://doi.org/10.1038/s41586-020-2149-4).
- [13] C. Bach, X. Dauchy, S. Etienne, Characterization of poly(ethylene terephthalate) used in commercial bottled water, *IOP Conf. Ser. Mater. Sci. Eng.* 5 (2009) 012005, doi:[10.1088/1757-899X/5/1/012005](https://doi.org/10.1088/1757-899X/5/1/012005).
- [14] P.G. Karagiannidis, A.C. Stergiou, G.P. Karayannidis, Study of crystallinity and thermomechanical analysis of annealed poly(ethylene terephthalate) films, *Eur. Polym. J.* 44 (2008) 1475–1486, doi:[10.1016/j.eurpolymj.2008.02.024](https://doi.org/10.1016/j.eurpolymj.2008.02.024).
- [15] Z. Chen, J.N. Hay, M.J. Jenkins, FTIR spectroscopic analysis of poly(ethylene terephthalate) on crystallization, *Eur. Polym. J.* 48 (2012) 1586–1610, doi:[10.1016/j.eurpolymj.2012.06.006](https://doi.org/10.1016/j.eurpolymj.2012.06.006).
- [16] R.M.R. Wellen, E. Canedo, M.S. Rabello, Nonisothermal cold crystallization of poly(ethylene terephthalate), *J. Mater. Res.* 26 (2011) 1107–1115, doi:[10.1557/jmr.2011.44](https://doi.org/10.1557/jmr.2011.44).
- [17] A. Mehta, U. Gaur, B. Wunderlich, Equilibrium melting parameters of poly(ethylene terephthalate), *J. Polym. Sci. Polym. Phys. Ed.* 16 (1978) 289–296, doi:[10.1002/pol.1978.180160209](https://doi.org/10.1002/pol.1978.180160209).
- [18] J. Arnling Bååth, K. Borch, P. Westh, A suspension-based assay and comparative detection methods for characterization of polyethylene terephthalate hydrolases, *Anal. Biochem.* 607 (2020), doi:[10.1016/j.ab.2020.113873](https://doi.org/10.1016/j.ab.2020.113873).
- [19] Z. Chen, J.N. Hay, M.J. Jenkins, The kinetics of crystallization of poly(ethylene terephthalate) measured by FTIR spectroscopy, *Eur. Polym. J.* 49 (2013) 1722–1730, doi:[10.1016/j.eurpolymj.2013.03.020](https://doi.org/10.1016/j.eurpolymj.2013.03.020).
- [20] T.W. Chan, A.I. Isayev, Quiescent polymer crystallization: modelling and measurements, *Polym. Eng. Sci.* 34 (1994) 461–471, doi:[10.1002/pen.760340602](https://doi.org/10.1002/pen.760340602).
- [21] E.Z.L. Zhong-Johnson, C.A. Voight, A.J. Sinskey, An absorbance method for analysis of enzymatic degradation kinetics of poly(ethylene terephthalate) films, *Sci. Rep.* 11 (2021) 928, doi:[10.1038/s41598-020-79031](https://doi.org/10.1038/s41598-020-79031).